Journal of Alloys and Compounds 509 (2011) 1101–1105

Contents lists available at ScienceDirect

Journal of Alloys and Compounds

journal homepage: www.elsevier.com/locate/jallcom

Effects of Sn-doping on the electrical and thermal transport properties of p-type Cerium filled skutterudites

Pengfei Qiu[a,b], Xun Shi[a,*], Xihong Chen[a], Xiangyang Huang[a], Ruiheng Liu[a,b], Lidong Chen[a]

[a] CAS Key Laboratory of Materials for Energy Conversion, Shanghai Institute of Ceramics, Chinese Academy of Sciences, 1295 DingXi Road, Shanghai 200050, China
[b] Graduate University of Chinese Academy of Sciences, Beijing 100049, China

ARTICLE INFO

Article history:
Received 19 July 2010
Received in revised form 2 September 2010
Accepted 3 September 2010
Available online 28 October 2010

Keywords:
Thermoelectric
Skutterudites
Point defects
Transport properties

ABSTRACT

p-type Sn-doped $CoSb_3$-based skutterudite compounds have been prepared using melting–quenching–annealing method and spark plasma sintering technique. Sn atoms in our samples are completely soluted on Sb-site with a fixed charge state and non-magnetic feature, providing a better choice to ascertain the effect of element doping at the $[Co_4Sb_{12}]$ framework on the electrical and thermal transport properties in p-type skutterudites. Doping Sn at the framework introduces additional ionized impurity scattering to affect the electron transport greatly. Similar electrical transport properties between $Ce_{0.2}Co_4Sb_{11.2}Sn_{0.8}$ and $Co_4Sb_{11}Sn_{0.6}Te_{0.4}$ suggest that Ce fillers contribute little to the valence band edge. Filling Ce into the voids and doping Sn at the framework introduce additional phonon resonant and point defect scattering mechanisms, thereby reducing lattice thermal conductivity remarkably. Moreover, our data suggest that combining these two effects is more effective to suppress lattice thermal conductivity through scattering broad range of phonons with different frequencies.

1. Introduction

Thermoelectric materials offer the possibility of converting waste heat into useful electrical energy. In the past decade, extensive interest in thermoelectric materials has been focused on $CoSb_3$-based skutterudite compounds [1,2], which has promising electrical transport properties. Binary $CoSb_3$ compound crystallizes as a body-centered-cubic structure (space group *Im*3) with two voids at the 2*a* positions (12 coordinated) in each unit cell. Filling the oversized voids with guest atoms (*e.g.*, alkalis, alkaline earths, rare earths, and others) [3–12] could reduce lattice thermal conductivity effectively, thereby enhancing thermoelectric properties. n-type filled skutterudites could be obtained through partially filling the void sites, thus the chemical formula could be written as $G_yCo_4Sb_{12}$, where G represents the guest atom and *y* is its filling fraction. p-type filled skutterudites compounds can be formed by either doping Fe at Co-site or replacing Sb atoms by Ge or Sn, which introduces excessive holes to the system to make the materials showing p-type conducting. In the previous studies, $G_yCo_{4-x}Fe_xSb_{12}$ compounds have been widely investigated and reported with outstanding thermoelectric performance [13–15]. However, up to now, only a little work was focused on Ge- or Sn-doped $G_yCo_4Sb_{12}$ [16–18]. Furthermore, their high temperature thermoelectric properties were scarcely reported.

Doping at $[Co_4Sb_{12}]$ framework creates point defects to scatter both electrons and thermal phonons. The understanding of the doping effect is of great importance for thermoelectric property optimization. However, it is very difficult to get a clear understanding in p-type $G_yCo_{4-x}Fe_xSb_{12}$ because of the subtle feature of Fe atoms. Yang et al. investigated Fe-doped $CoSb_3$ and found that the valence state of Fe (Fe^{2+}/Fe^{3+}) varies with different doping content [19], which influences the electrical and thermal transport properties remarkably. Moreover, increasing Fe-doping content led to an increase in the vacancy concentration at the Co-site [19]. The vacancies, as well as the disordered Fe/Co site, would reduce thermal conductivity simultaneously, thus making it more difficult to understand the low lattice thermal conductivity observed in p-type $G_yCo_{4-x}Fe_xSb_{12}$ [13,14]. In addition, the uncertain magnetic effect introduced by Fe atoms would also influence the thermoelectric properties. Therefore, doping Ge or Sn at Sb-site might be a good choice to get clear understanding of the doping effect at the skutterudite framework due to their stable valence state as well as non-magnetic feature.

In this study, we choose doping Sn at Sb-site instead of Fe at Co-site to prepare p-type filled skutterudites. Polycrystalline $Ce_yCo_4Sb_{12-x}Sn_x$ ($x = 0, 0.8, 1.1$, $y = 0, 0.11, 0.2$) samples were synthesized and their electrical and thermal transport properties were investigated. Although Yb-filled skutterudites have been reported having excellent thermoelectric performance [9], in this work, Ce is used as the filling element with the purpose to avoid the unpredictable effect by the uncertain valence state (Yb^{2+}/Yb^{3+}) of Yb on the thermoelectric properties [18,20]. One

* Corresponding author.
E-mail address: ylxshi@gmail.com (X. Shi).

0925-8388/$ – see front matter © 2010 Elsevier B.V. All rights reserved.
doi:10.1016/j.jallcom.2010.09.162

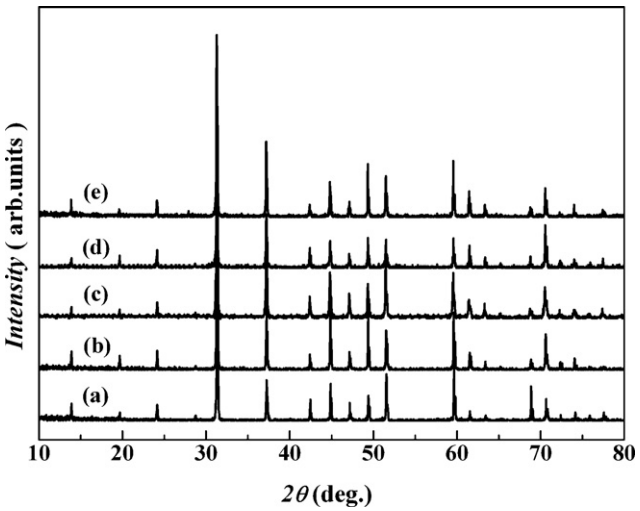

Fig. 1. X-ray diffraction patterns for $Ce_yCo_4Sb_{12-x}Sn_x$: (a) $x=0$, $y=0$; (b) $x=0$, $y=0.11$; (c) $x=0.8$, $y=0.2$; (d) $x=1.1$, $y=0.2$; and (e) $Co_4Sb_{11}Sn_{0.6}Te_{0.4}$ samples.

sample, $Co_4Sb_{11}Sn_{0.6}Te_{0.4}$ with Sn and Te co-doped at Sb-site, was also prepared for comparison.

2. Experimental

High pure raw elements were weighed in the atomic ratio and sealed in evacuated quartz ampoules with coated carbon. The sealed ampoules were heated slowly up to 1350 K for 10 h, then quenched into water bath, and annealed at 973–1073 K for 7 days. To form densified pellets, the obtained ingots were ground into fine powder and then sintered by Spark Plasma Sintering (SPS) at 773–853 K for 10–15 min. High-density (>95% of the theoretical density) was achieved in all samples. To examine the purity and chemical composition of the samples, X-ray diffraction (XRD) analysis (Rigaku, Rint2000) and electron probe microanalysis (EPMA, Shimadzu 8705QH2) were employed. Electrical transport properties, including electrical conductivity (σ) and Seebeck coefficient (S) were measured using the ZEM-3 (ULVAC Co. Ltd.) apparatus under Helium atmosphere from 300 to 750 K. Thermal conductivity was calculated using the measured values of thermal diffusivity, specific heat and sample density. The thermal diffusivity and specific heat were measured in argon atmosphere using laser flash method (NETZSCH LFA 427) and Shimadzu DSC-50, respectively. The density of the samples was measured using the Archimedes method. Hall coefficients (R_H) were measured in a Physical Property Measurement System (Quantum Design) by sweeping the magnetic field up to 3 T in both positive and negative directions. In a single carrier model, the Hall carrier concentration is equal to $1/R_He$, where e is the elementary charge. The Hall carrier mobility (μ_H) was calculated according to the relation $\mu_H = R_H\sigma$.

3. Results and discussion

3.1. XRD and lattice constant

Fig. 1 shows the powder XRD patterns for all samples. All the peaks are identified to show $CoAs_3$ structure. No Sn-included impurities were observed. EPMA analysis confirmed that the actual Ce filling fraction is similar with the nominal composition. Therefore, in this paper, the nominal compositions will be used for all the samples. Doping Sn at the Sb-site would compensate the electrons donated by Ce fillers, and thereby increasing the maximum Ce filling fraction. The lattice constant (a) of all samples is shown in Table 1. $Ce_{0.11}Co_4Sb_{12}$ shows larger a than that in pure $CoSb_3$. Doping Sn at Sb-site would further enlarge the lattice volume because the ion radius of Sn^{4-} (0.294 nm) is larger than that of Sb^{3-} (0.245 nm) [21].

3.2. Carrier concentration and mobility

Fig. 2(a) shows the temperature dependence of carrier concentration (n for electrons, p for holes) for all samples. At 300 K, n is $3.6\times10^{17}\,cm^{-3}$ and $9.1\times10^{19}\,cm^{-3}$ for n-type $CoSb_3$ and

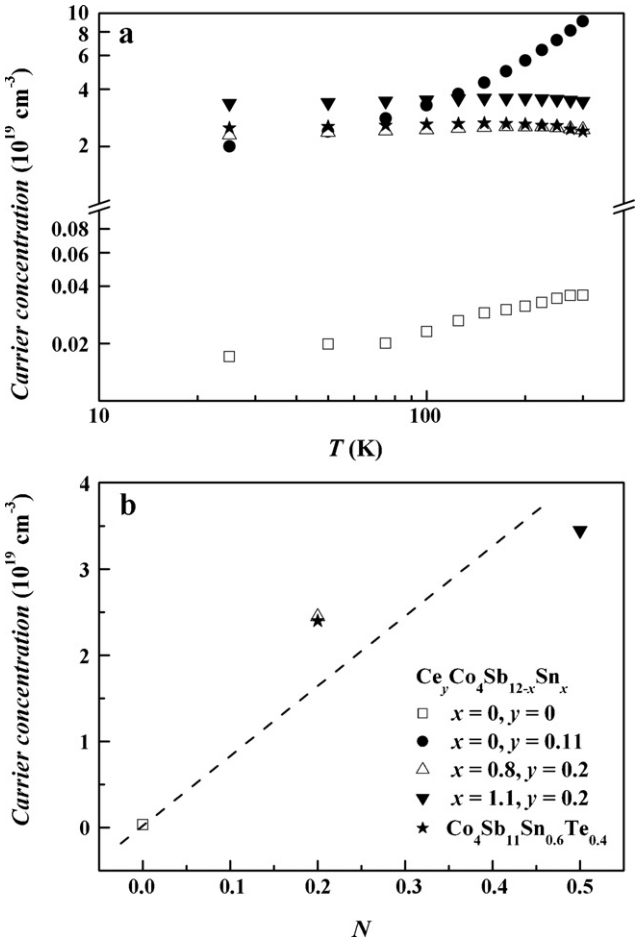

Fig. 2. (a) Temperature dependence of carrier concentration for all samples. (b) carrier concentration as a function of the effective hole numbers for all samples.

$Ce_{0.11}Co_4Sb_{12}$, respectively. The donated electrons by Ce fillers are responsible for the remarkable increase of n in $Ce_{0.11}Co_4Sb_{12}$. Because Sn is one electron less than Sb, doping Sn at Sb-site introduces excessive holes into the $[Co_4Sb_{12}]$ framework, and changes the materials into p-type conducting. Therefore, p would increase with increasing Sn content (shown in Fig. 2(a)). Sn-doped samples exhibit weak temperature dependences, indicating that they are all heavily doped semiconductors.

For $Ce_yCo_4Sb_{12-x}Sn_x$ skutterudites, we can estimate the effective hole numbers (N) in a unit cell using simple charge accounting. In filled-skutterudites, filler Ce donates its valence electrons to the framework and the effective charge state is reported around +3 [4,14]. Since Sn is one electron less than Sb, the effective charge state of Sn in skutterudites should be close to −1. Therefore, N is equal to $(x-3y)$. Positive $(x-3y)$ indicates the major carrier is holes, while negative value corresponds to electrons. For instance, in $Ce_{0.2}Co_4Sb_{11.2}Sn_{0.8}$, $N=(0.8-0.2\times3)=0.2$, thereby it shows p-type conducting, consistent with our hall measurement. Fig. 2(b) shows the experimental Hall carrier concentration as a function of N for all samples. Obviously, experimental Hall carrier concentration increases with increasing N. Since Te is one electron more than Sb, the calculated N number is also 0.2 in $Co_4Sb_{11}Sn_{0.6}Te_{0.4}$ using the method mentioned above. Therefore, the measured hole concentration in $Co_4Sb_{11}Sn_{0.6}Te_{0.4}$ is expected similar as that in $Ce_{0.2}Co_4Sb_{11.2}Sn_{0.8}$. Sample $Co_4Sb_{11}Sn_{0.6}Te_{0.4}$ is also included in Fig. 2(b), and it has almost the same N and hole concentration as $Ce_{0.2}Co_4Sb_{11.2}Sn_{0.8}$, following well with the trend. Furthermore, our results further confirm that Sn atoms are completely soluted at Sb sites with a fixed charge state.

Table 1
Lattice constant, and some physical properties at room temperature for $Ce_yCo_4Sb_{12-x}Sn_x$ and $Co_4Sb_{11}Sn_{0.6}Te_{0.4}$ samples.

	Co_4Sb_{12}	$Ce_{0.11}Co_4Sb_{12}$	$Ce_{0.2}Co_4Sb_{11.2}Sn_{0.1}$	$Ce_{0.2}Co_4Sb_{10.9}Sn_{1.1}$	$Ce_4Sb_{11}Te_{0.4}$
Lattice parameter a (nm)	0.90368	0.90419	0.90487	0.90579	0.90482
Electrical conductivity σ ($\times 10^4$ S m^{-1})	0.00683	7.32	6.79	7.68	6.95
Seebeck coeeficient S (μV/K)	−438.5	−190.7	16.8	15.9	13.2
Hall carrier concentration ($\times 10^{19}$ cm^{-3})	0.0359	9.07	2.45	3.45	2.40
Hall mobility μ_H (cm^2/V s^{-1})	123.47	51.18	176.95	118.94	176.59

Fig. 3 shows the temperature dependence of Hall mobility (μ_H) for all samples. μ_H for $Ce_{0.2}Co_4Sb_{11.2}Sn_{0.8}$ (174 cm^2/V s at 300 K), is about one order of magnitude higher than that in p-type Fe-doped $G_yCo_4Sb_{12}$ [13]. Doping Sn into skutterudites instead of Fe could avoid the effect of the localized 3d states and the mixed charge state of Fe atoms on the electrical transports, thereby improving the carrier motilities. For pure $CoSb_3$, μ_H follows a $T^{3/2}$ dependence near room temperature, suggesting that ionized impurity scattering dominates the carrier transport. Mandrus et al. reported that acoustic phonon scattering can be neglected in pure $CoSb_3$ at low temperature due to the low n and light carrier effective mass [22]. μ_H of $Ce_{0.11}Co_4Sb_{12}$ follows a $T^{-3/2}$ dependence near room temperature, indicating that acoustic phonon scattering is the predominant scattering mechanism. Actually, μ_H of all $G_yCo_4Sb_{12}$ compounds with different filling elements or filling fractions agree quite well with $T^{-3/2}$ dependence near room temperature [3,6,23]. In $G_yCo_4Sb_{12}$, [Co_4Sb_{12}] framework is generally regarded as electrically conducting pathway [24]. Thus, although the filling atoms in the voids are electron donor, they scarcely introduce additional ionized impurity scattering or affect the electron transport. However, the case is totally different for the samples with element doping at the [Co_4Sb_{12}] framework. As shown in Fig. 3, μ_H of all Sn-doped samples decreases much slowly with increasing temperature. The doped Sn at the framework with a negative charge state could act as ionized impurities to scatter carriers greatly. Therefore, near room temperature, the predominant scattering mechanism for Sn-doped samples is a combination of acoustic phonon scattering and ionized impurity scattering. The similar phenomenon has been reported in Ni-doped n-type $Ba_yCo_{4-x}Ni_xSb_{12}$ [6] and transition-metal doped type-I clathrates [25].

3.3. Electrical transport properties

Fig. 4 shows the temperature dependence of electrical conductivity (σ) and Seebeck coefficient (S) for all samples. Except pure $CoSb_3$, σ for all samples decreases with increasing temperature, indicating typical heavily doped semiconducting behavior. For pure $CoSb_3$, an intrinsic transition is observed and the sign of S is changed from negative to positive around 400 K due to the rise of minor carriers. S for all Sn-doped samples is relatively low as compared with those in n-type skutterudites. Dilley et al. suggested that doping Sn into the skutterudites creates a broad Sn p-band near Fermi level (E_F) which screens the contribution of the other bands, and thereby deteriorates S [16]. This point of view is consistent with our electronic structure calculation for $Co_4Sb_{11}Sn_1$ compound (Unpublished results). $Ce_{0.2}Co_4Sb_{11.2}Sn_{0.8}$ possesses lower σ than $Ce_{0.2}Co_4Sb_{10.9}Sn_{1.1}$ due to the low carrier concentration. However, the magnitude and temperature dependences of S for the two samples are almost the same, although their Sn concentrations are different with each other. Similar phenomena are also observed in the low temperature study of n-type $Yb_yCo_4Sb_{12-x}Sn_x$ by Yang et al. [17]. The broad Sn p-band near E_F might be related to this abnormal behavior.

Interestingly, $Ce_{0.2}Co_4Sb_{11.2}Sn_{0.8}$ exhibits similar σ and S with $Co_4Sb_{11}Sn_{0.6}Te_{0.4}$ in the whole temperature range investigated here. Combined with the similar Hall carrier concentration and mobility mentioned above, it suggested that Ce atoms may scarcely affect the valence band edge at this low carrier density. This picture might be reasonable since E_F in $Ce_{0.2}Co_4Sb_{11.2}Sn_{0.8}$ sample with low hole density should be close to the band edge while

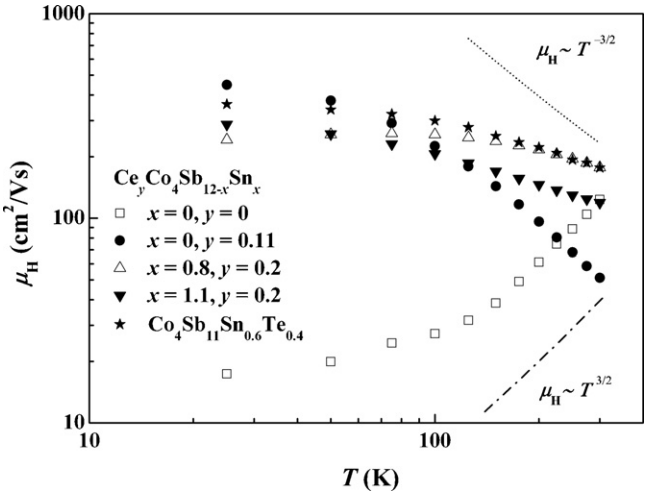

Fig. 3. Temperature dependence of Hall carrier mobility for all samples. The dash doted line and dot line show $T^{3/2}$ and $T^{-3/2}$ dependence, respectively.

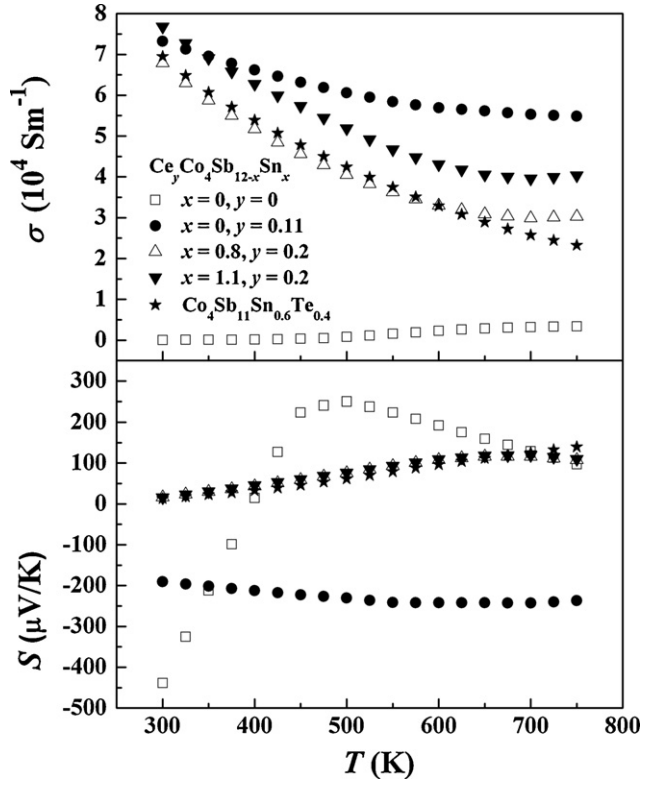

Fig. 4. Temperature dependence of electrical conductivity and Seebeck coefficient for all samples.

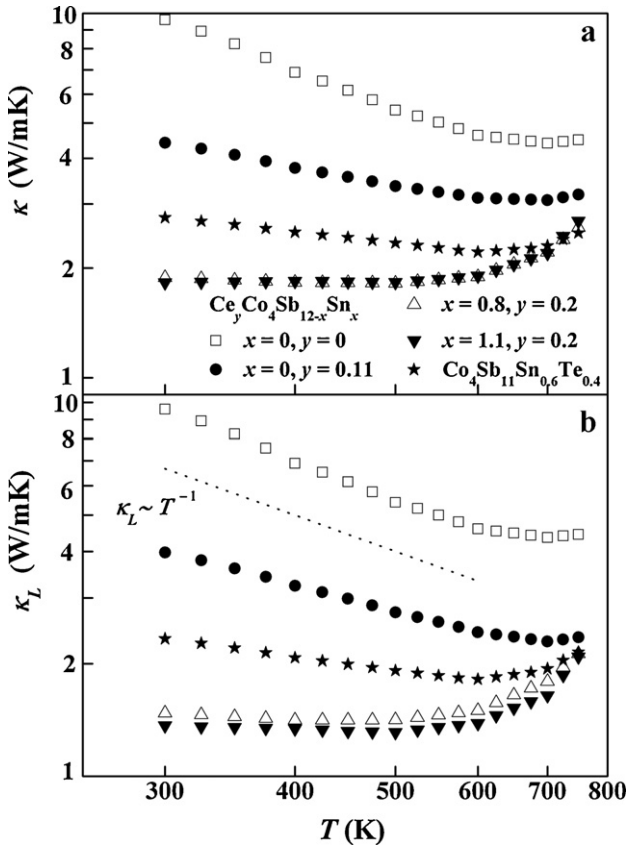

Fig. 5. Temperature dependence of (a) thermal conductivity and (b) lattice thermal conductivity for all samples. The dot line shows a T^{-1} dependence expected from purely phonon–phonon scattering.

usually the localized Ce-4f bands are sitting in the deep of the bands.

3.4. Thermal transport properties

Fig. 5(a) shows the temperature dependence of thermal conductivity (κ) for all samples. The value of κ initially decreases with increasing temperature, reaches a minimum number around 650 K, then increases as temperature increases. The turning point implies the start of bipolar diffusion as a result of intrinsic excitation. Usually, the total thermal conductivity is a sum of two contributions: lattice part κ_L and carrier part κ_c. κ_c can be estimated by the Wiedemann–Franz law as $\kappa_c = L_0\sigma T$, where L_0 is the Lorenz number (2.0×10^{-8} V^2/K^2). Fig. 5(b) shows the calculated κ_L by subtracting κ_c from κ. κ_L for pure $CoSb_3$ is very large, while $Ce_yCo_4Sb_{12-x}Sn_x$ samples show rather low κ_L as compared with other samples. Filling guest atoms and doping other atoms into skutterudites could scatter lattice phonons, and thereby reduce κ_L significantly. Generally, phonon scattering mechanism in solids includes (1) grain boundary scattering, (2) point-defect scattering, (3) phonon–phonon (Umklapp processes) scattering, and (4) electron–phonon scattering [26]. For filled skutterudites, phonon resonant scattering by the fillers also need to be taken into account [17]. At high temperature ($T > \Theta_D$, where Θ_D is the Debye temperature), grain boundary scattering and electron-phonon scattering can be ignored without changing any physical trend. In addition, the effects of phonon resonance scattering and point-defect scattering on suppressing κ_L are more obvious at low temperature than at high temperature. As shown in Fig. 5(b), κ_L for pure $CoSb_3$ follows a T^{-1} dependence below 600 K, indicating phonon–phonon scattering is the predominant phonon scattering mechanism [27]. For Ce-filled samples, Ce "rattles" in the voids and introduces additional phonon resonance scattering, resulting in a small slope of the κ_L versus T curve shown in Fig. 5(b). Further smaller slope is observed for sample $Co_4Sb_{11}Sn_{0.6}Te_{0.4}$ because both Sn and Te at skutterudites create extra point defects on the framework to strongly scatter phonons, thereby changing the dominated phonon scattering mechanism. For $Ce_{0.2}Co_4Sb_{11.2}Sn_{0.8}$ and $Ce_{0.2}Co_4Sb_{10.9}Sn_{1.1}$, κ_L is nearly independent with the temperature, which should be attributed to the combined effect of Ce-filling and Sn-doping.

At 300 K, κ_L for $Ce_{0.2}Co_4Sb_{11.2}Sn_{0.8}$ is 1.4 W/m K, merely 37% of that in $Ce_{0.11}Co_4Sb_{12}$. High Ce filling fraction in $Ce_{0.2}Co_4Sb_{11.2}Sn_{0.8}$ definitely results in lower κ_L. However, compared with other $G_yCo_4Sb_{12}$ skutterudites with higher filling fraction [3–5], κ_L in $Ce_{0.2}Co_4Sb_{11.2}Sn_{0.8}$ is still much lower, indicating a significant κ_L reduction by Sn atoms at skutterudite framework. Furthermore, as shown in Fig. 5(b), κ_L decreases with increasing Sn content, further confirming that Sn plays an important role in the reduction of κ_L. In the inelastic resonant phonon scattering model, only those phonons with frequencies close to the localized rattling frequency of filling atoms can be scattered by phonon resonant scattering [28,29]. Doping Sn at Sb-site could create large amount of point defects to scatter high frequency lattice phonons. This type of phonon scattering is different from the phonon resonant scattering introduced by the fillers, where the low or middle frequency phonons is strongly scattered. Therefore, combining both the effects of filling guest atoms and doping other elements into the skutterudites, different phonon scattering modes could be realized to scatter a broad range of lattice phonons, thereby strongly decreasing κ_L. Moreover, Sn-doped samples show much lower κ_L than that of Fe-doped samples [13–15]. Rotter et al. investigated the lattice dynamics of $CoSb_3$ using inelastic X-ray scattering and they found that the low frequency phonons mainly correspond to vibrations of Sb atoms rather than Co atoms [30]. Therefore, doping other elements at Sb-site is believed more effective to scatter phonons than doping at Co-site, which is consistent with and confirmed by our results.

4. Conclusions

In this study, p-type skutterudites $Ce_yCo_4Sb_{12-x}Sn_x$ have been prepared and the effects of Sn-doping on the electrical and thermal transport properties were studied. Sn-doping supplies holes to the $[Co_4Sb_{12}]$ framework to make the materials showing p-type conducting. Hall carrier concentration results suggest that Sn is completely soluted at Sb-site in the samples, consistent with our XRD and EPMA measurements that no Sn-included impurities were observed. μ_H of all Sn-doped samples are rather higher than that of Fe-doped p-type skutterudites, suggesting that doping Sn into skutterudites instead of Fe could avoid the adverse effects of the localized 3d states and mixed charge state of Fe atoms on μ_H. Doping Sn at Sb-site creates additional point defects at $[Co_4Sb_{12}]$ framework, thereby enhancing ionized impurity scattering to carriers to affect the electron transports greatly. With increasing Sn-doped content, σ increases while S remains almost unchanged. The broad Sn p-band near E_F may account for these results. $Ce_{0.2}Co_4Sb_{11.2}Sn_{0.8}$ possesses similar electrical transport properties as $Co_4Sb_{11}Sn_{0.6}Te_{0.4}$, indicating that the Ce fillers in p-type skutterudites scarcely influence the valence band edge. Both Ce-filling and Sn-doping could reduce κ_L remarkably by introducing additional phonon resonant and point defect scattering mechanisms. Our results show that the combination of effects of filling guest atoms into the voids and doping other elements at the framework in skutterudites might be more effective to suppress κ_L through scattering a broader range of phonons with different frequencies.

Acknowledgments

This work was partly supported by National Natural Science Foundation of China (Contract No. 50802109, 50820145203), and the Knowledge Innovation Program of the Chinese Academy of Sciences (Contract No. KJCX2-YW-H20).

References

[1] C. Uher, Proceedings of the 21st International Conference on Thermoelectrics, IEEE, Piscataway, NJ, 2001, pp. 35–41.
[2] L.D. Chen, Z. Xiong, S.Q. Bai, J. Inorg. Mater. 25 (2010) 00561–00568.
[3] Y.Z. Pei, J. Yang, L.D. Chen, W. Zhang, J.R. Salvador, J. Yang, Appl. Phys. Lett. 95 (2009) 042101.
[4] X. Shi, W. Zhang, L.D. Chen, J. Yang, C. Uher, Phys. Rev. B 75 (2007) 235208.
[5] L.D. Chen, T. Kawahara, X.F. Tang, T. Goto, T. Hirai, J.S. Dyck, W. Chen, C. Uher, J. Appl. Phys. 90 (2001) 1864–1868.
[6] J.S. Dyck, W. Chen, C. Uher, L.D. Chen, X.F. Tang, T. Hirai, J. Appl. Phys. 91 (2002) 3698–3705.
[7] Y.P. Jiang, X.P. Jia, T.C. Su, N. Dong, F.R. Yu, Y.J. Tian, W. Guo, H.W. Xu, L. Deng, H.A. Ma, J. Alloys Compd. 493 (2010) 535–538.
[8] D.T. Morelli, G.P. Meisner, B.X. Chen, S.Q. Hu, C. Uher, Phys. Rev. B 56 (1997) 7376.
[9] G.S. Nolas, M. Kaeser, R.T. Littleton, T.M. Tritt, Appl. Phys. Lett. 77 (2000) 1855–1857.
[10] G.A. Lamberton Jr., S. Bhattacharya, R.T. Littleton, M.A. Kaeser, R.H. Tedstrom, T.M. Tritt, J. Yang, G.S. Nolas, Appl. Phys. Lett. 80 (2002) 598–600.
[11] B.C. Sales, B.C. Chakoumakos, D. Mandrus, Phys. Rev. B 61 (2000) 2475.
[12] G.S. Nolas, H. Takizawa, T. Endo, H. Sellinschegg, D.C. Johnson, Appl. Phys. Lett. 77 (2000) 52–54.
[13] X.F. Tang, Q.J. Zhang, L.D. Chen, T. Goto, T. Hirai, J. Appl. Phys. 97 (2005) 093712.
[14] X.F. Tang, L.D. Chen, J. Wang, Q.J. Zhang, T. Goto, T. Hirai, J. Alloys Compd. 394 (2005) 259–264.
[15] G. Rogl, A. Grytsiv, E. Bauer, P. Rogl, M. Zehetbauer, Intermetallics 18 (2010) 57–64.
[16] N.R. Dilley, E.D. Bauer, M.B. Maple, B.C. Sales, J. Appl. Phys. 88 (2000) 1948–1951.
[17] J. Yang, D.T. Morelli, G.P. Meisner, W. Chen, J.S. Dyck, C. Uher, Phys. Rev. B 67 (2003) 165207.
[18] F. Grandjean, G. Long, B. Mahieu, J. Yang, G.P. Meisner, D.T. Morelli, J. Appl. Phys. 94 (2003) 6683–6691.
[19] J. Yang, G.P. Meisner, D.T. Morelli, C. Uher, Phys. Rev. B 63 (2000) 014410.
[20] F. Grandjean, G.J. Long, R. Cortes, D.T. Morelli, G.P. Meisner, Phys. Rev. B 62 (2000) 12569.
[21] R.D. Shannon, Acta Cryst. A32 (1976) 751–767.
[22] D. Mandrus, A. Migliori, T.W. Darling, M.F. Hundley, E.J. Peterson, J.D. Thompson, Phys. Rev. B 52 (1995) 4926.
[23] S.Q. Bai, Y.Z. Pei, L.D. Chen, W.Q. Zhang, X.Y. Zhao, J. Yang, Acta Mater. 57 (2009) 3135–3139.
[24] M.L. Liu, I.W. Chen, F.Q. Huang, L.D. Chen, Adv. Mater. 21 (2009) 3808–3812.
[25] X. Shi, J. Yang, S.Q. Bai, J.H. Yang, H. Wang, M.F. Chi, J.R. Salvador, W.Q. Zhang, L.D. Chen, W. Wong-Ng, Adv. Funct. Mater. 20 (2010) 755–763.
[26] H. Anno, K. Matsubara, Y. Notohara, T. Sakakibara, H. Tashiro, J. Appl. Phys. 86 (1999) 3780–3786.
[27] G.S. Nolas, J. Sharp, H.J. Goldsmid, Thermoelectrics: Basic Principles and New Materials Developments, Springer, Berlin, 2001, p. 76.
[28] J. Yang, W. Zhang, S.Q. Bai, Z. Mei, L.D. Chen, Appl. Phys. Lett. 90 (2007) 192111.
[29] X. Shi, H. Kong, C.-P. Li, C. Uher, J. Yang, J.R. Salvador, H. Wang, L. Chen, W. Zhang, Appl. Phys. Lett. 92 (2008) 182101.
[30] M. Rotter, P. Rogl, A. Grytsiv, W. Wolf, M. Krisch, A. Mirone, Phys. Rev. B 77 (2008) 144301.